Influence of the film properties on the plasma etching dynamics of rf-sputtered indium zinc oxide layers

L. Stafford,[a] W. T. Lim, and S. J. Pearton
Department of Materials Science and Engineering, University of Florida, Gainesville, Florida 32611

M. Chicoine, S. Gujrathi, and F. Schiettekatte
Département de Physique, Université de Montréal, Montréal, Québec H3C 3J7, Canada

Jae-Soung Park, Ju-Il Song, Young-Woo Heo, Joon-Hyung Lee, and Jeong-Joo Kim
Department of Inorganic Materials Engineering, Kyungpook National University, Daegu 702-701, Korea

I. I. Kravchenko
Department of Physics, University of Florida, Gainesville, Florida 32611

(Received 10 November 2006; accepted 9 April 2007; published 14 May 2007)

The etching characteristics of indium zinc oxide (IZO) films were investigated using a high-density plasma in Ar, Ar/Cl_2, and $Ar/CH_4/H_2$ chemistries. The IZO layers were deposited by means of rf magnetron sputtering, in which the target composition and growth temperature were varied to selectively tune the film properties. X-ray diffraction, elastic recoil detection, and Rutherford backscattering spectroscopy were used to determine the crystallization quality, atomic density, and composition of the as-deposited IZO films. As the In/(In+Zn) composition ratio in the IZO layer increases, the etch yield in Ar and Ar/Cl_2 plasmas remains fairly constant, indicating that the etching dynamic is essentially independent of the film properties. In sharp contrast, a strong increase of the IZO etch yield with the In/(In+Zn) fraction is observed in $Ar/CH_4/H_2$ plasma due to the preferential desorption of the group-III etch products. By comparing these experimental data to the predictions of a simple rate model accounting for preferential desorption effects, it is concluded that the balance between etching and polymer deposition in the $Ar/CH_4/H_2$ plasma plays an important role in the evolution of the IZO etch rate with the In concentration fraction. © *2007 American Vacuum Society.* [DOI: 10.1116/1.2736679]

I. INTRODUCTION

Because of their high electrical conductivity and high optical transparency, transparent conducting oxides (TCOs) have been extensively studied for transparent electrodes in various optoelectronic devices such as liquid-crystal displays, solar cells, and light-emitting diodes (LEDs).[1–11] Although $SnO_2-In_2O_3$ (ITO) is the most commonly used TCO for transparent electrodes,[12] there is significant interest in developing new alternatives to this material because the scarcity of indium imparts a very high cost to ITO.[13] To this end, numerous studies on binary, ternary, or even quaternary compound oxides composed of combinations of In, Zn, Cd, Sn, and Ga have been reported in the literature.[14–27] Among these materials, the In_2O_3-ZnO (IZO) system has attracted a lot of attention because of the absence of toxic cadmium and the use of inexpensive zinc. In addition, compared to ITO, IZO layers are characterized by a larger work function[13,28] and a superior transmission in the $1-1.5$ μm range.[29] Promising results on the use of IZO films for fabricating Ohmic contacts to *n*-type ZnO for LED applications were also recently reported.[30]

So far, IZO films have been prepared by metal organic chemical vapor deposition,[31] sputtering,[32–34] pulsed-laser deposition,[35] and sol-gel.[36] Although the growth characteristics of IZO layers are relatively well understood, the development of a reliable pattern transfer process for IZO is still in its infancy. Among the various patterning techniques, plasma etching is preferred because it allows high-resolution pattern transfer for device structures. Recently, the etch rate of IZO films in Ar/Cl_2 and $Ar/CH_4/H_2$ plasma chemistries was shown to be influenced by the plasma characteristics such as reactive neutral density, positive ion density, and ion energy.[37] However, in addition to the plasma parameters, it is also expected that the film properties somewhat impact the etching characteristics.

In this work, we investigate the influence of the film properties on the plasma etching dynamics of IZO layers through an extensive characterization. We first examine the effect of the target composition and deposition temperature on the properties of rf-sputtered IZO layers using x-ray diffraction (XRD), elastic recoil detection (ERD), and Rutherford backscattering spectroscopy (RBS). Based on this full characterization, it is shown that although the etch rates in Ar and Ar/Cl_2 plasmas are independent of both the crystallization quality and film composition, the etching characteristics in $Ar/CH_4/H_2$ chemistries strongly depend on the In concentration fraction.

II. EXPERIMENTAL SETUP

IZO films were deposited on glass substrates (Corning EAGLE2000) using rf magnetron sputtering. The

[a]Electronic mail: sluc@mse.ufl.edu

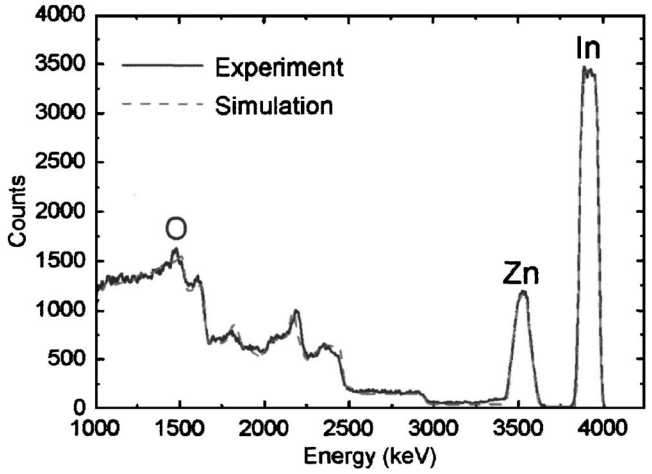

FIG. 1. RBS spectra from the IZO film grown using the $In_2O_3(ZnO)_4$ target under room-temperature conditions. A SIMNRA simulation is also shown for comparison.

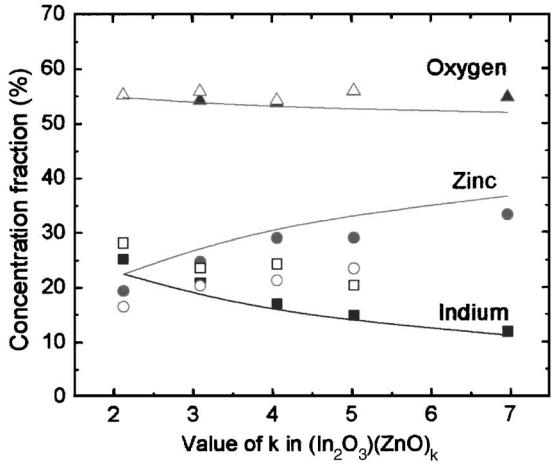

FIG. 2. Concentration fraction of O, Zn, and In atoms in the as-deposited IZO layers obtained by RBS. The full symbols are for RT deposition, whereas the open ones correspond to IZO films deposited at 500 °C. The composition of the target (full line) is also shown for comparison.

$In_2O_3(ZnO)_k$ targets, where $k=2$, 3, 4, 5, and 7, were fabricated using high-purity In_2O_3(99.99%) and ZnO(99.9%) by a conventional ceramic processing technique.[38] The substrates were cleaned in an ultrasonic bath with trichloroethylene, acetone, and ethanol prior to loading in the deposition chamber. The base pressure of the chamber was $\sim 10^{-7}$ Torr. The target was presputtered for 10 min before growth. Sputtering was carried out at an argon pressure of 10 mTorr with a sputtering power of 50 W. The distance between the target and substrate was fixed at 70 mm. The deposition temperature was varied from room temperature (RT) to 500 °C. XRD (Mac Science, M03XHF) was used to examine the crystallization quality. The composition of each sample was analyzed by RBS using a 4.57 MeV $^4He^{++}$ ion beam at normal incidence. The angle between the He beam and the surface normal was 7° to minimize channeling. The detector was placed at a scattering angle of 170°. The RBS spectra were then analyzed using SIMNRA simulations to take into account the non-Rutherford cross section on oxygen.[39] The results of this fit provided the concentration fraction of each element and the atomic density of the film integrated over the layer thickness. To obtain the atomic density N_t, the integrated atomic density was divided by the film thickness measured by a KLA-Tencor surface profilometer. For further analysis, ERD measurements were also performed using a 40 MeV Co^+ ion beam at normal incidence. More details on the ERD technique and spectra analysis can be found elsewhere.[40,41]

High-density plasma etching of IZO films was realized using an Oerlikon (formerly UNAXIS) 790 inductively coupled plasma (ICP) reactor. The 2 MHz power applied to the ICP source and the rf (13.56 MHz) chuck power were held constant at 300 and 200 W, respectively. Etching was performed in Ar, Ar/Cl_2, and $Ar/CH_4/H_2$ chemistries. The Ar concentration in Ar/Cl_2 and $Ar/CH_4/H_2$ was controlled by varying the Ar mass flow rate between 0 and 20 sccm (SCCM denotes cubic centimeter per minute at STP), while keeping the Cl_2 and CH_4/H_2 mass flow rates constant (10 SCCM Cl_2 for Ar/Cl_2; 3 SCCM CH_4 and 10 SCCM H_2 for $Ar/CH_4/H_2$). The total gas pressure before plasma ignition was set to 5 mTorr. The IZO etch rate was determined from stylus profilometry measurements. During the current experiments, the plasma exposure time was set to 2 min for investigations realized in $Ar/CH_4/H_2$ and 5 min for those performed in Ar and Ar/Cl_2.

III. RESULTS AND DISCUSSION

A. Film properties

Figure 1 presents a typical RBS spectrum obtained from the IZO layer grown using a $In_2O_3(ZnO)_4$ target under RT conditions. The peaks observed in Fig. 1 correspond to O, Zn, and In, respectively, the O peak being superimposed to the broad glass substrate contribution. The results of the SIMNRA simulations are also shown for comparison. To account for the substrate contribution in the simulations, the back side of the sample was analyzed to determine the composition of the glass substrate. As mentioned above, N_t can be determined by dividing the areal atomic density obtained from the fit by the film thickness. For all samples, we found $N_t \approx 82 \pm 5$ nm^{-3}. This value is very similar to that expected from bulk, single-crystal IZO. For example, for $In_2O_3(ZnO)_4$, the volume of the IZO lattice is 162 Å^3 with 13 atoms per unit cell, which yields $N_t = 80$ nm^{-3}.

The results for the concentration fraction of each element in the IZO films are displayed in Fig. 2 as a function of the k value in the $In_2O_3(ZnO)_k$ target. The composition of the target is also shown for comparison. For both growth temperatures investigated, the Zn content is lower than that in the target, with this difference being larger for IZO films grown at 500 °C. This may result from a lower sticking coefficient and/or a higher vapor pressure of Zn compared to that of In. Figure 2 further shows that the oxygen content is fairly in-

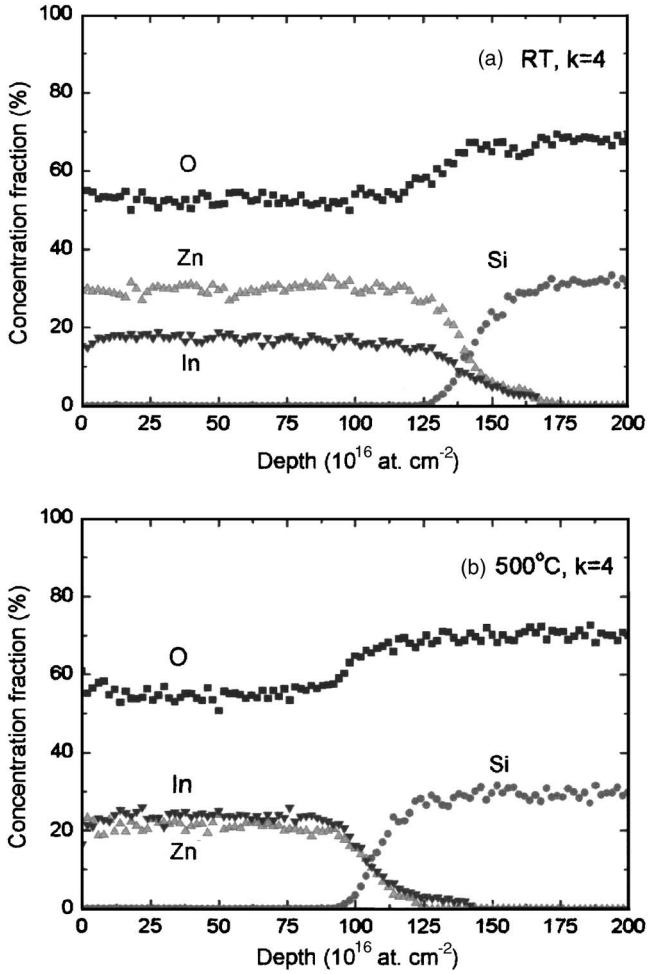

FIG. 3. Depth profiles obtained from the ERD measurements for IZO films grown using the $In_2O_3(ZnO)_4$ target at either (a) room temperature or (b) 500 °C.

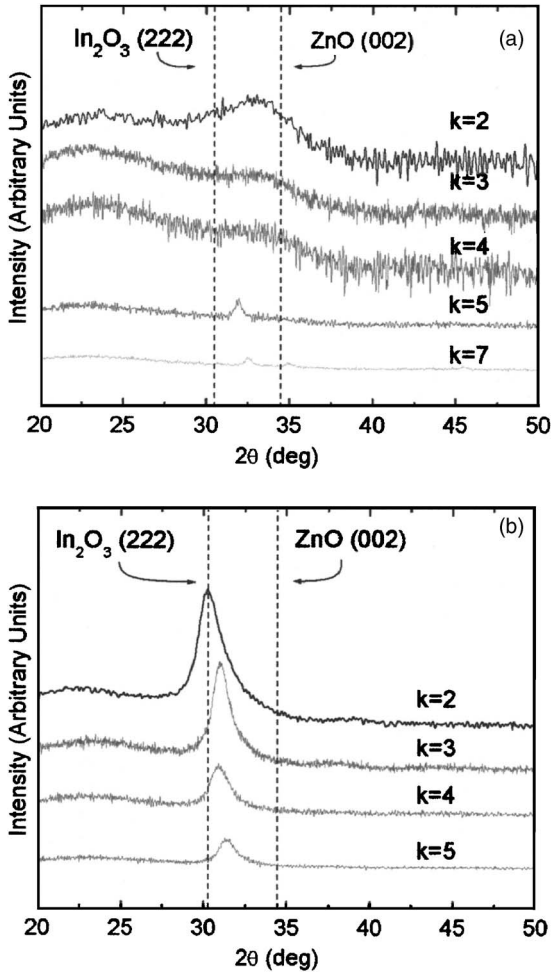

FIG. 4. XRD spectra from IZO films deposited at either (a) room temperature or (b) 500 °C.

dependent of the k value in both RT- and 500 °C-deposited IZO layers, with these values being similar to those expected from the target composition.

Because the O peak in the RBS spectra is weak and superimposed to the broad glass substrate contribution, there could be some errors in our determination of the O concentration. For validation, we have compared our RBS results to those of ERD. This technique is known to be more suitable for the analysis of light elements such as O in solids containing heavy atoms such as Zn and In. The results obtained for IZO films grown using the $In_2O_3(ZnO)_4$ target at either RT or 500 °C are shown in Fig. 3 as typical examples. It can be seen that the concentration fractions of Zn and In in RT-deposited IZO films are about 29% and 17%, respectively, in excellent agreement with the results obtained by RBS. As for oxygen, the concentration fraction is 53±2%, which is also similar to the RBS results (54+2%). Figure 3 further shows that the depth profiles are smooth, with a relatively thick interface. Indeed, in both cases, the thickness of the interfacial region is about 35×10^{16} at. cm^{-2}, which corresponds to an actual thickness of 40±5 nm.

Changes in the target composition can also induce modification of the microstructural properties of the film. To illustrate this behavior, Fig. 4 presents the influence of the k value in the $In_2O_3(ZnO)_k$ target on the XRD spectra of IZO layers deposited at either RT [Fig. 4(a)] or 500 °C [Fig. 4(b)]. The films grown at RT are essentially amorphous for $k\leqslant4$, whereas a small peak can be seen for $k=5$ and $k=7$. On the other hand, for IZO films grown at 500 °C, Fig. 4(b) shows a broad peak between 30.5° and 32.3°, which indicates that the films are crystalline and textured. According to Dupont *et al.*,[42] the broad XRD peak of IZO layers can be related to a distribution of In_2O_3 and $In_2O_3(ZnO)_k$ polytypes. The films grown using the $k=2$ target show the lowest overall peak position at 30.5°, with this position being linked to the (222) plane of In_2O_3. For higher k values, the overall XRD peak is shifted toward higher diffraction angles. These higher 2θ values can be attributed to the (00l) reflections of the $In_2O_3(ZnO)_k$ compounds.

B. Etching characteristics

Figure 5 presents the influence of the In concentration fraction on the sputter-etch yield of IZO films obtained in a

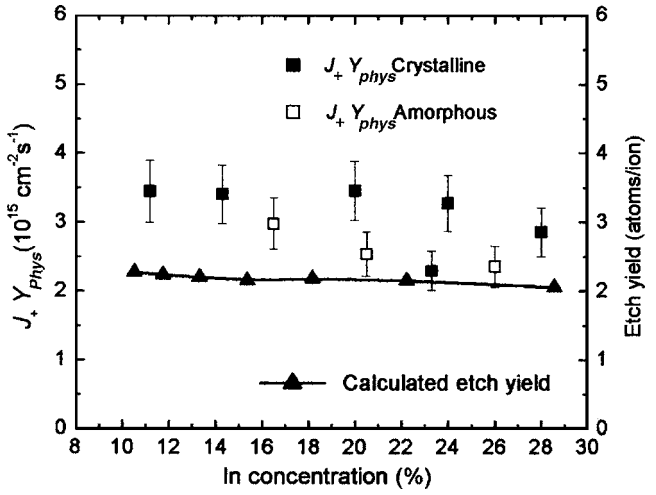

FIG. 5. Influence of the indium concentration fraction on the sputter-etch yield of IZO films obtained in a pure argon plasma. The full symbols are for RT deposition, whereas the open ones correspond to IZO films deposited at 500 °C. The results from our Monte Carlo simulations are also shown for comparison.

pure argon atmosphere. The sputter-etch yield Y_{phys} can be determined from $\text{ER}=J_+Y_{\text{phys}}/N_t$, where ER is the sputter-etch rate and J_+ is the positive ion flux impinging onto the material surface. As the exact value of J_+ is unknown for the plasma under investigation, J_+Y_{phys} is displayed in Fig. 5 instead of Y_{phys}. Within the uncertainties, J_+Y_{phys} is seen to be independent of both the crystallization quality and composition of the IZO films. In Ref. 43, it was shown that the sputter-etching characteristics of pulsed-laser-deposited $SrTiO_3$ films can be influenced by the film microstructural properties. In particular, it was found that polycrystalline $SrTiO_3$ layers grown under relatively high oxygen background pressure present an atomic density much lower than that expected from bulk, single-crystal $SrTiO_3$ due to the presence of micropores within grain boundaries. For this latter system, the sputter-etch rate was found to be inversely proportional to the film atomic density, whereas the sputter-etch yield was constant for all deposition conditions. By comparison, the atomic densities of the IZO films investigated in the present work are similar independently of the growth conditions, and as a consequence, the sputter-etch rate and the sputter-etch yield are independent of both the crystallization quality and film composition.

We have compared our experimental results for the sputter-etch yield to those predicted by Monte Carlo simulations.[44] For these simulations, we used the mass densities calculated from the RBS results. The binding energies used in the present simulations are those provided by the software. These values are listed in Table I. The energy of the argon ions was kept constant at 300 eV, which is similar to the value expected from the sum of bias voltage (−275 V) and sheath potential (−25 V) in the experiments. The results of our simulations are shown on the right axis of Fig. 5. It can be seen that the sputter-etch yield decreases only slightly with increasing In concentration fraction, with the mean value being 2.2±0.2 atoms/ion. This dependence of the calculated etch yield is in very good agreement with that deduced from the experimental data. On the other hand, assuming that J_+ is in the typical 10^{16} cm^{-2} s^{-1} range for inductively coupled argon plasmas operated at low pressure,[43] we estimate $Y_{\text{phys}} \sim 0.3$ from the experimental data presented in Fig. 5. Our experimental results are thus lower than those predicted by the Monte Carlo simulations. Among the possible explanations, this discrepancy is likely to result from the redeposition of sputtered species following their interaction with the gas phase, resulting in a lower effective sputter-etch yield. Indeed, it was shown that the degree of redeposition of sputtered metals such as Pt and complex oxides such as $(Ba,Sr)TiO_3$ and $SrBiTa_2O_9$ reaches ~90% in the 5–15 mTorr range.[45–47]

TABLE I. Binding energies used in the Monte Carlo simulations.

	In	Zn	O
Displacement energy (eV)	25	25	28
Lattice binding energy (eV)	3	3	3
Surface binding energy (eV)	2.49	1.35	2

Figure 6 presents the influence of the In concentration fraction on the normalized sputter-etch yield of O, In, and Zn obtained from the Monte Carlo simulations. This normalized sputter-etch yield was calculated according to

$$\text{Normalized etch yield} = (Y_j/Y_{\text{tot}})/\xi_j, \tag{1}$$

where Y_j is the etch yield of the element j, Y_{tot} is the total etch yield (i.e., $Y_O+Y_{Zn}+Y_{In}$), and ξ_j is the concentration fraction of the element j in the as-deposited IZO films. Over the whole range of In concentration investigated, the normalized etch yield of Zn is found to be higher than 1. It is also higher than those of In and O by about a factor of 2. This indicates that during sputter etching of IZO layers by noble argon ions, there is preferential sputtering of the Zn atoms.

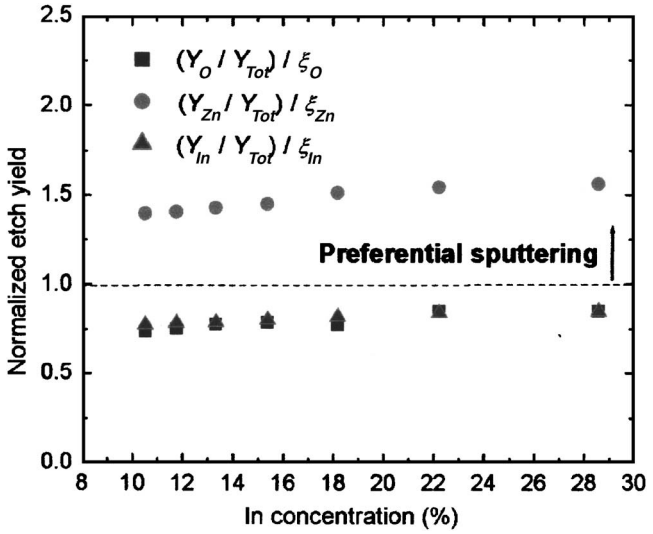

FIG. 6. Influence of the indium concentration on the normalized sputter-etch yield of IZO films.

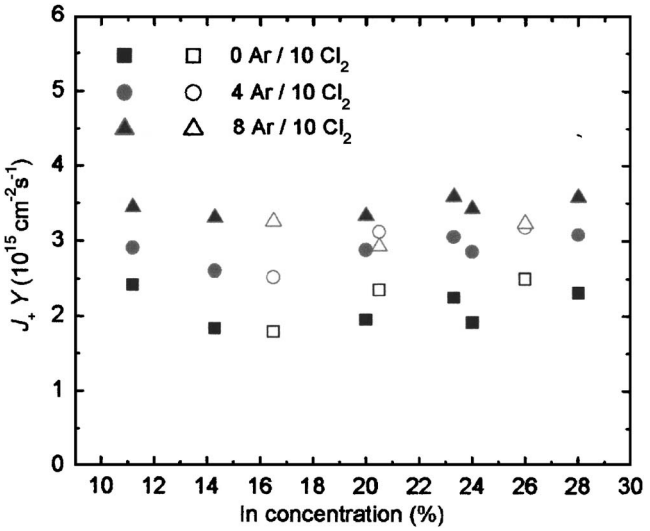

FIG. 7. Influence of the indium concentration on the etch yield of IZO films obtained in Ar/Cl_2 plasmas. The full symbols are for RT deposition, whereas the open ones correspond to IZO films deposited at 500 °C.

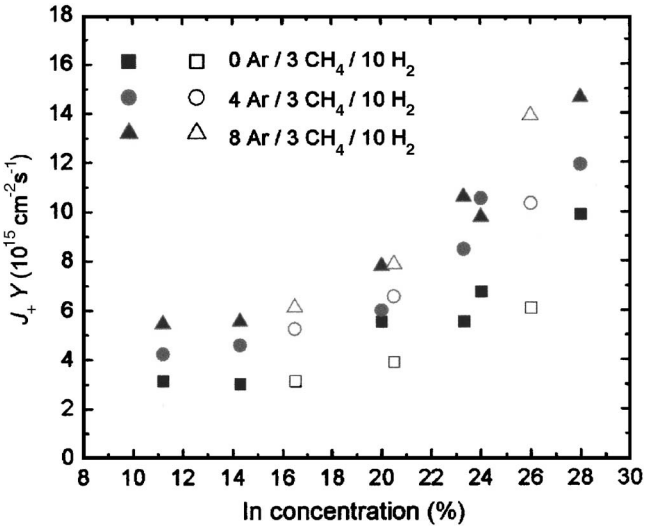

FIG. 8. Influence of the indium concentration on the etch yield of IZO films obtained in $Ar/CH_4/H_2$ plasmas. The full symbols are for RT deposition, whereas the open ones correspond to IZO films deposited at 500 °C.

This result is in excellent agreement with our previous Auger electron spectroscopy measurements that showed a Zn-depleted IZO surface following sputter etching in a pure argon plasma.[37]

The influence of the indium concentration fraction on the etch yield of IZO layers in Ar/Cl_2 plasmas is shown in Fig. 7. Over the whole range of Ar concentrations investigated, the etch yield is seen to be similar for both amorphous and crystalline IZO layers. In addition, the IZO etch yield is independent of the film composition within experimental errors. Figure 7 further shows that J_+Y increases with the Ar concentration. Assuming that the etch rate is ion-flux limited,[37] i.e., $ER = J_+ Y_{sat}/N_t$, where Y_{sat} is the ion-assisted chemical etch yield on an IZO surface saturated with reactive neutrals; the higher J_+Y values can be attributed to the expected higher positive ion flux.[48–51]

Figure 8 presents the influence of the indium concentration fraction on the etch yield of IZO films in $Ar/CH_4/H_2$ plasma. As in Figs. 5 and 7, there are no differences within the uncertainties between the etch yield of amorphous and crystalline IZO layers. Nevertheless, the IZO etch yields in $Ar/CH_4/H_2$ are, on the average, much higher than those presented in Figs. 5 and 7 for Ar and Ar/Cl_2 plasmas. In a previous paper, it was found that the depth profile of IZO layers after etching in $CH_4/H_2/Ar$ plasmas presents a relatively thick In-depleted region, in which the Zn concentration fraction largely exceeds that in as-deposited IZO films.[37] The higher etch yields displayed in Fig. 8 can therefore be understood from the preferential desorption of In-containing reaction products. Figure 8 further shows that the IZO etch yield increases only slightly at low indium concentration and then strongly increases beyond 17%. Similar results are obtained for all Ar concentrations in $Ar/CH_4/H_2$ investigated, with the etch yield simply increasing with the Ar concentration.

To gain further insights into the meaning of our results, we developed a simple rate model accounting for preferential etching effects. Generally, the etch yield of a multicomponent material can be written as the sum of the etch yields of each elements. Indeed, despite possible variations in the surface composition upon preferential etching, conservation of mass implies that for sufficiently long etching times, the fraction of the etch yield of each element is given by its concentration fraction in the material.[52] Therefore, for IZO films, one can write

$$Y = \sum_i \xi_i Y_i = \xi_O Y_O + \xi_{Zn} Y_{Zn} + \xi_{In} Y_{In}. \quad (2)$$

Since $\xi_O + \xi_{Zn} + \xi_{In} = 1$, Eq. (2) can then be rewritten as

$$Y = \xi_O Y_O + (1 - \xi_O - \xi_{In}) Y_{Zn} \left(1 + \frac{\xi_{In} Y_{In}}{(1 - \xi_O - \xi_{In}) Y_{Zn}} \right). \quad (3)$$

For the IZO films investigated in the present work, Fig. 2 has shown that ξ_O is approximately the same, independent of the target composition and growth temperature. Thus, for given plasma etching conditions, the only variable in Eq. (3) is ξ_{In}.

We calculated the etch yield of the IZO films as a function of the In concentration fraction using Eq. (3). The results are shown in Fig. 9 for two (Y_{In}, Y_O, Y_{Zn}) calculation sets. Set 1 is $Y_{In} = Y_O = 1$; $Y_{Zn} = 2$. This set of individual etch yields is based on the normalized etch yields deduced from the Monte Carlo simulations for physical sputtering with Ar ions displayed in Fig. 6. In this framework, the calculated IZO etch yield is seen to only slightly decrease with increasing In concentration, in excellent agreement with both the experimental data and the simulations shown in Fig. 5. The dependence of the etch yield on ξ_{In} obtained from this set of calculations is also similar to the experimental data for IZO etching in Ar/Cl_2 plasmas presented in Fig. 7. This suggests that the relative values for the individual etch yields in the Ar/Cl_2 plasma are similar to those in a pure argon atmo-

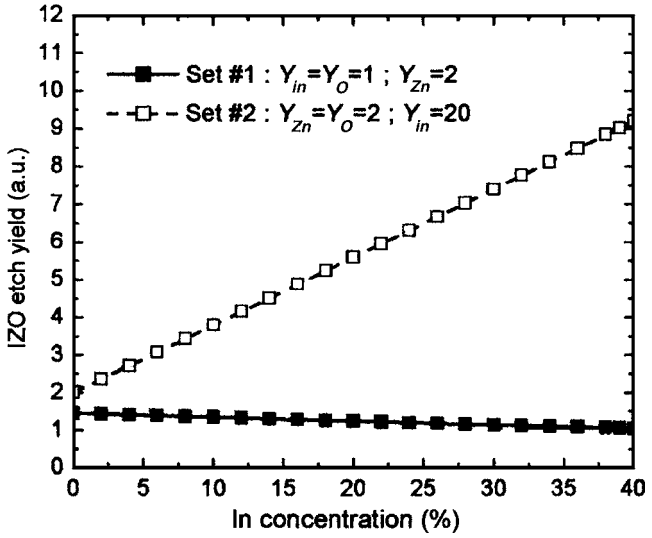

FIG. 9. Influence of the indium concentration on the calculated IZO etch yield.

sphere, in excellent agreement with the similar surface composition reported previously.[37] Note that in the Cl_2 plasma, one would expect a very high fragmentation level of the Cl_2 molecules for the high-power-density conditions investigated.[53] As a consequence, Cl^+ should be the dominant chlorine charge carrier.[54,55] Because the mass of Cl^+ is close to that of Ar^+, the energy transferred by the incident ions through nuclear collisions in the material is similar for both ions, thereby yielding comparable individual etch yields.

Set 2 is $Y_{Zn}=Y_O=2$; $Y_{In}=20$. This set of etch yields corresponds to a situation where there is preferential desorption of In, as expected for IZO etching in $Ar/CH_4/H_2$ plasmas (see Fig. 8). In this case, Fig. 9 shows a linear increase of the IZO etch yield with increasing ξ_{In}. However, this linear dependence differs from that of the experimental data presented in Fig. 8, with the latter exhibiting a smoother variation at low In concentrations. This difference in the etch yield behavior can probably be attributed to the formation of the polymer layer during etching in methane-containing plasmas. Indeed, after ignition of the plasma, CH_x deposition takes place on the IZO surface. Ion bombardment then results in breaking bonds and mixing of the near-surface region, and, thus, in the formation and release of the reaction products.[56–58] However, due to the significant difference in the desorption rates of In- and Zn-containing reaction products, the rate of CH_x consumption by the IZO layer will depend on the In concentration fraction, resulting in different balances between etching and deposition for the various IZO layers.[59] This mechanism is not considered in the simple model presented above. Therefore, in the presence of polymer deposition, additional physics is required to adequately simulate the influence of the film composition on the etching characteristics of IZO layers.

IV. CONCLUSION

In this work, we examined the influence of the film properties on the plasma etching dynamics of IZO films in Ar, Ar/Cl_2, and $Ar/CH_4/H_2$ plasmas. In all plasma conditions investigated, the etching characteristics were found to be independent of the film crystallization quality. As the In/(In+Zn) composition ratio in the IZO layer increases, the etch yield in Ar and Ar/Cl_2 plasmas remained approximately the same, in excellent agreement with both Monte Carlo simulations and the predictions of a simple rate model accounting for preferential etching effects. In sharp contrast, a strong increase of the IZO etch yield with the In/(In+Zn) fraction was observed in $Ar/CH_4/H_2$ plasma because of the preferential desorption of the group-III etch products. However, for this latter system, it was suggested that the balance between IZO etching and polymer deposition plays an important role in predicting the evolution of the IZO etch rate with the indium concentration fraction.

ACKNOWLEDGMENTS

One of the authors (L.S.) would like to acknowledge the financial support from the postdoctoral fellowship program of the Natural Science and Engineering Research Council (NSERC). This research was sponsored by the Army Research Office under Grant No. DAAD19-01-1-0603, the National Science Foundation under Grant Nos. DMR0400416 and 0305228 (L. Hess), the Department of Energy (DOE) under Grant No. DE-FC26-04NT42271, the DOE Contract No. DE-AC05-00OR22725, and by the Air Force Office of Scientific Research under Grant No. F49620-03-1-0370. This was also supported by the National Research Laboratory grant from the Ministry of Science and Technology and Korea Science and Engineering Foundation. The work at Université de Montréal was supported by NSERC and by the Fonds Québécois de la Recherche sur la Nature et les Technologies.

[1] A. Shah, P. Torres, R. Tscharner, N. Wyrsch, and H. Keppner, Science **285**, 692 (1999).
[2] H. K. Kim, K. S. Lee, and J. H. Kwon, Appl. Phys. Lett. **88**, 012103 (2006).
[3] K. Ramamoorthy, K. Kumar, R. Chandramohan, and K. Sankaranarayanan, Mater. Sci. Eng., B **126**, 1 (2006).
[4] D. S. Ginley and C. Bright, MRS Bull. **25**, 15 (2000).
[5] R. H. Franken, C. H. M. Van der Werf, J. Löffler, J. K. Rath, and R. E. I. Schropp, Thin Solid Films **501**, 47 (2006).
[6] Y. H. Tak, K. B. Kim, H. G. Park, K. H. Lee, and J. R. Lee, Thin Solid Films **411**, 12 (2002).
[7] C. D. Tsai, C. H. Fu, Y. J. Lin, and C. T. Lee, Solid-State Electron. **43**, 665 (1999).
[8] W. Wohlmolth, M. Arafa, P. Fay, and I. Abesida, Appl. Phys. Lett. **70**, 3026 (1997).
[9] S. H. Kang, D. K. Hwang, and S. J. Park, Appl. Phys. Lett. **86**, 211902 (2005).
[10] G. Hu, B. Kumar, H. Gong, E. F. Chor, and P. Wu, Appl. Phys. Lett. **88**, 101901 (2006).
[11] T. L. Breen, P. M. Frayer, R. W. Nunes, and M. E. Rothwell, Langmuir **18**, 194 (2002).
[12] I. Hamberg and C. G. Granqvist, J. Appl. Phys. **60**, R123 (1986).
[13] T. Minami, MRS Bull. **25**, 38 (2000).
[14] K. Nomura *et al.*, J. Appl. Phys. **95**, 5532 (2004).
[15] D. D. Edwards, T. O. Mason, F. Goutenoire, and K. R. Poeppelmeier,

Appl. Phys. Lett. **70**, 1706 (1997).
[16]B. Yaglioglu, H. Y. Yeom, and D. C. Paine, Appl. Phys. Lett. **86**, 261908 (2005).
[17]J. D. Perkins *et al.*, Thin Solid Films **411**, 152 (2002).
[18]G. B. Palmer and K. R. Poeppelmeier, Springer Ser. Solid-State Sci. **4**, 317 (2002).
[19]T. Minami, T. Miyata, and T. Yamamoto, Surf. Coat. Technol. **108–109**, 583 (1998).
[20]K. Ramamoorthy, K. Kumar, R. Chandramohan, and K. Sankaranarayanan, Mater. Sci. Eng., B **126**, 1 (2006).
[21]N. Ito, Y. Sato, P. K. Song, A. Kaijio, K. Inoue, and Y. Shigesato, Thin Solid Films **496**, 99 (2006).
[22]Y. S. Jung, J. Y. Seo, D. W. Lee, and D. Y. Jeon, Thin Solid Films **445**, 63 (2003).
[23]N. Naghavi, A. Rougier, C. Marcel, C. Guery, J. B. Leriche, and J. M. Tarascon, Thin Solid Films **360**, 233 (2000).
[24]N. Ito, Y. Sato, P. K. Song, A. Kaijio, K. Inoue, and Y. Shigesato, Thin Solid Films **496**, 99 (2006).
[25]Y. S. Jung, J. Y. Seo, D. W. Lee, and D. Y. Jeon, Thin Solid Films **445**, 63 (2003).
[26]N. Naghavi, A. Rougier, C. Marcel, C. Guery, J. B. Leriche, and J. M. Tarascon, Thin Solid Films **360**, 233 (2000).
[27]W. J. Lee *et al.*, Solid-State Electron. **46**, 477 (2002).
[28]J. Cui, A. Wang, N. L. Edleman, J. Ni, P. Lee, N. R. Armstrong, and T. J. Marks, Adv. Mater. (Weinheim, Ger.) **31**, 1476 (2001).
[29]J. M. Phillips *et al.*, Appl. Phys. Lett. **67**, 2246 (1995).
[30]G. Hu, B. Kumar, H. Gong, E. F. Chor, and P. Wu, Appl. Phys. Lett. **88**, 101901 (2006).
[31]A. Wang, J. Dai, J. Cheng, M. P. Chudzik, T. J. Marks, R. P. H. Chang, and C. R. Kannewurf, Appl. Phys. Lett. **73**, 327 (1998).
[32]K. Tominaga, T. Takao, A. Fukushima, T. Moriga, and I. Nakabayashi, Vacuum **66**, 505 (2002).
[33]T. Minami, T. Kakumu, Y. Takeda, and S. Takata, Thin Solid Films **290–291**, 1 (1996).
[34]T. Minami, T. Kakumu, Y. Takeda, and S. Takata, Thin Solid Films **317**, 326 (1998).
[35]N. Naghavi, C. Marcel, L. Dupont, A. Rougier, J. B. Leriche, and C. Guery, J. Mater. Chem. **10**, 2315 (2000).
[36]S. Y. Lee and B. O. Park, Thin Solid Films **484**, 184 (2005).
[37]W. T. Lim, L. Stafford, J.-I. Song, J.-S. Park, Y. W. Heo, J.-H. Lee, J.-J. Kim, and S. J. Pearton, Appl. Surf. Sci. **253**, 2752 (2006).
[38]K. Y. Son, D. H. Park, J. H. Lee, J. J. Kim, and J. S. Lee, Solid State Ionics **172**, 425 (2004).
[39]M. Mayer, AIP Conf. Proc. **475**, 541 (1999).
[40]R. Grouleau, S. C. Gujrathi, and J.-P. Martin, Nucl. Instrum. Methods Phys. Res. **218**, 11 (1983).
[41]F. Schiettekatte, Nucl. Instrum. Methods Phys. Res. B **219–220**, 430 (2004).
[42]L. Dupont, C. Maugy, N. Naghavi, C. Guery, and J.-M. Tarascon, J. Solid State Chem. **158**, 119 (2001).
[43]L. Stafford, M. Gaidi, M. Chaker, O. Langlois, J. Margot, F. Schiettekatte, and P. Wei, Appl. Phys. Lett. **84**, 2500 (2004).
[44]J. F. Ziegler, J. P. Biersack, and U. Littmark, *The Stopping and Range of Ions in Solids* (Pergamon, New York, 1985).
[45]S. Delprat, M. Chaker, and J. Margot, J. Appl. Phys. **89**, 29 (2001).
[46]L. Stafford, J. Margot, S. Delprat, M. Chaker, and D. Queney, J. Vac. Sci. Technol. A **20**, 530 (2002).
[47]L. Stafford, J. Margot, S. Delprat, M. Chaker, and S. J. Pearton, J. Appl. Phys. (to be published).
[48]L. Stafford, J. Margot, O. Langlois, and M. Chaker, J. Vac. Sci. Technol. A **21**, 1247 (2003).
[49]L. Jiang, N. O. V. Plank, M. A. Blauw, R. Cheung, and E. van der Drift, J. Phys. D **37**, 1809 (2004).
[50]H. S. Kima, G. Y. Yeoma, J. W. Leeb, and T. I. Kim, Thin Solid Films **341**, 180 (1999).
[51]J. R. Woodworth, M. E. Riley, P. A. Miller, C. A. Nichols, and T. W. Hamilton, J. Vac. Sci. Technol. A **15**, 3015 (1997).
[52]M. Nastasi, J. M. Mayer, and J. K. Hirvoven, *Ion-Solid Interactions: Fundamentals and Applications* (Cambridge University Press, Cambridge, 1996), Chap. 9, pp. 230–235.
[53]M. V. Malyshev and V. M. Donnelly, J. Appl. Phys. **88**, 6207 (2000).
[54]L. Stafford, J. Margot, F. Vidal, M. Chaker, K. Giroux, J. S. Poirier, A. Quintal-Leonard, and J. Saussac, J. Appl. Phys. **98**, 063301 (2005).
[55]M. V. Malyshev, N. C. M. Fuller, K. H. A. Bogart, V. M. Donnelly, and I. P. Herman, Appl. Phys. Lett. **74**, 1666 (1999).
[56]M. E. Barone and D. B. Graves, J. Appl. Phys. **78**, 6604 (1995).
[57]D. Humbird and D. B. Graves, J. Vac. Sci. Technol. A **23**, 31 (2005).
[58]L. Stafford, S. J. Pearton, and J. Margot, J. Appl. Phys. **100**, 063309 (2006).
[59]M. Schaepkens, T. E. F. M. Standaert, N. R. Rueger, P. G. M. Sebel, G. S. Oehrlein, and J. M. Cook, J. Vac. Sci. Technol. A **17**, 26 (1999).